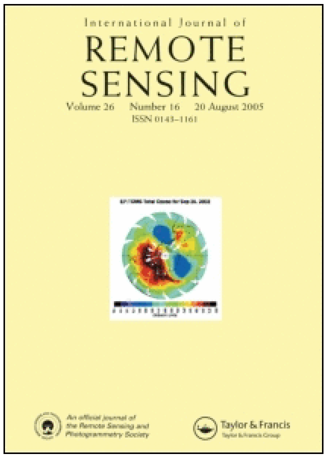

International Journal of Remote Sensing
Publication details, including instructions for authors and subscription information:
http://www.informaworld.com/smpp/title~content=t713722504

Remote sensing of the water attenuation in coral reefs: a case study in French Polynesia

S. Maritorena [a]
[a] Université Française du Pacifique, Laboratoire d'Ecologie Marine. Tahiti. French Polynesia

Online Publication Date: 01 January 1996
To cite this Article: Maritorena, S. , (1996) 'Remote sensing of the water attenuation in coral reefs: a case study in French Polynesia', International Journal of Remote Sensing, 17:1, 155 - 166
To link to this article: DOI: 10.1080/01431169608948992
URL: http://dx.doi.org/10.1080/01431169608948992

INT. J. REMOTE SENSING, 1996, VOL. 17, NO. 1, 155–166

Remote sensing of the water attenuation in coral reefs: a case study in French Polynesia

S. MARITORENA

Université Française du Pacifique, Laboratoire d'Ecologie Marine, BP 6570—Faaa/Aéroport, Tahiti, French Polynesia

(Received 11 July 1994; in final form 6 January 1995)

Abstract. The diffuse attenuation coefficient is an essential parameter of a semi-analytical model of radiances used to process a remotely-sensed image for bottom mapping of coral reefs in French Polynesia. Spectral and wide-band values (SPOT-XS-1 and XS-2 and Landsat TM-1) of the diffuse attenuation coefficient were computed from *in situ* spectral irradiances measured with an underwater spectroradiometer in the ocean and in the lagoonal waters of two islands in French Polynesia. These data show that emerged zones may strongly influence attenuation, mainly at short wavelengths. Attenuation was also assessed statistically in two different ways from a SPOT image of the island of Bora Bora. This image was then processed to obtain a map of the bottom corrected for water column effects.

1. Introduction

The social and economic importance of coral reefs is obvious to all insular Indo-Pacific states and the increasing anthropic stress on these environments involves better basic mapping, monitoring and management. To a certain extent, remote sensing can contribute to these tasks. The use of satellite imagery in the study of coral reefs started at the end of the 1970s with the Landsat MSS data (see e.g., Bina *et al.* 1978, Jupp *et al.* 1981 a, b, 1985, Lyzenga 1981). Since the appearance of a new generation of high spatial resolution satellites (Landsat or SPOT) the benefit of the previous sensors was somehow limited in coral reef studies because of their poor spatial resolution. These new tools were soon considered to be able to offer better performances in applications such as bathymetry estimation and bottom recognition. This is particularly true in French Polynesia where reef features are mainly made up of small scale patterns. Moreover, remote sensing techniques are of practical interest in French Polynesia because of the very wide geographical distribution of the islands (120 high islands or atolls spread over a 2·5 million km^2 area of the South Pacific Ocean).

In shallow water zones, one of the problems encountered when using remote imagery comes from the fact that the measured radiances depend on the reflection properties of the bottom and on the effect of the water above it (for a complete description of these effects (see e.g., Gordon and Brown 1974, Spitzer and Dirks 1987, Philpot 1989, Maritorena *et al.* 1994). By using a simple water radiance model, Lyzenga (1978, 1981) showed how the contribution of the bottom and of the water column could be processed separately. The method proposed by Lyzenga is based on the knowledge of the diffuse attenuation coefficient of the water in the wavebands used. The present paper deals with this particular point for waters in French Polynesia and some aspect associated with the use of remote sensing of coral reefs.

2. Theoretical background

The method discussed here makes use of an approximate expression that gives the value of any radiometric quantity at the surface as a function of the reflection properties of the bottom, the depth of the bottom and an optical property of the water (i.e., the exponential decay model). As this expression does not take into account all the phenomena influencing the signal, such a model can be considered as semi-analytical. This model is discussed elsewhere in a detailed manner (Maritorena *et al.* 1994) and can be expressed for radiance or irradiance at sea level as follows:

$$L_i(H) = L_{i\infty} + (A_i - L_{i\infty})\, e^{-2K_i H} \qquad (1)$$

where the subscript i stands for the wavelength or the spectral band considered, $L_i(H)$ is the radiance measured just under the surface when the bottom is at depth H, $L_{i\infty}$ is the radiance of an infinitely deep ocean, A_i is the albedo of the bottom, K_i is an attenuation term and H is the depth of the bottom. In practice, K_i can be replaced by K_d the diffuse attenuation coefficient for downwelling irradiance (see Maritorena *et al.* 1994).

When $L_{i\infty}$ is known and subtracted from $L_i(H)$, (1) can be linearized by a simple natural logarithm transformation. This results in a set of equations of the form:

$$X_i = \ln(L_i - L_{i\infty}) \qquad (2)$$

In a X_i versus X_j co-ordinate system, the points corresponding to radiances emerging from the same kind of bottom located at various depths are linearly related and the different kinds of bottoms are represented by parallel linear functions. In such a two-dimensional representation, each kind of bottom is approximately represented by a linear function with a slope equal to K_i/K_j, i.e., the rato of the diffuse attenuation coefficient in spectral bands i and j. Lyzenga (1981) showed that this slope can be obtained from the symmetry axis of the scatterplot. When K_i/K_j is known, this ratio can be used to obtain two quantities, one being linearly related to depth and the other, independent of the depth, which can be considered as an index of the kind of bottom. These new variables can be obtained through simple rotation of the system axis, the range of this rotation being given by $\tan^{-1}(K_i/K_j)$.

This rotation or, more generally, the ratio K_i/K_j is a critical point in this method as the accuracy of depth estimation or bottom recognition depends on it. This particular point will now be examined in the case of waters encountered in the lagoons of French Polynesia.

3. Optical properties of the water column from *in situ* data

In order to obtain $K(\lambda)$, spectral downwelling irradiances were measured at different depths for 21 stations in French Polynesia: in the lagoon and above the outer reef slope in Moorea (Society archipelago) and in the lagoon in Takapoto atoll (Tuamotu archipelago) (figure 1). Measurements were recorded between 400 and 700 nm using a Li-Cor UW1800 underwater spectroradiometer. At each station, $K(\lambda)$ is obtained from the downwelling irradiances at two different depths according to:

$$K_d(\lambda)(z_1, z_2) = \frac{1}{z_2 - z_1} \ln \frac{E_d(\lambda, z_1)}{E_d(\lambda, z_2)} \qquad (3)$$

where z is the depth (with $z_2 > z_1$) and $E_d(\lambda,z)$ is the downwelling irradiance at depth z and wavelength λ.

The reflectances at zero depth, $R^{\infty}(0-, \lambda)$, given by the ratio of the upwelling irradiance just under the surface, $E_u(0-, \lambda)$ to the downwelling irradiance at the same depth, $E_d(0-, \lambda)$, were also computed.

In lagoonal waters, optical properties depend upon the presence of organic and inorganic particulate and dissolved matter. As phytoplankton biomass is generally low in coral reef lagoons of French Polynesia (typically 0·1 to 0·3 mg m^{-3}, see e.g., Sournia and Ricard 1976, Charpy and Charpy-Roubaud, 1991, Delesalle and Sournia 1992), its influence on optical properties of the waters remains weak. Other particulate materials and dissolved matter appear to have a predominant role in most cases (Blanchot *et al.* 1989). These latter influences are of course stronger in high island waters because of larger terrestrial run-offs, regulated by the amount of rainfall.

These variable influences can be observed on mean diffuse attenuation coefficients and reflectances for the two islands (figure 2). At all wavelengths, Moorea shows higher attenuation than Takapoto indicating a better clarity of the water in the lagoon of the atoll. The greatest differences in attenuation between Moorea and Takapoto occur at short wavelengths (K(400 nm) = 0·16 m^{-1} and 0·11 m^{-1} respectively) mainly because of increased absorption caused by a higher particulate and dissolved matter load in the Moorea lagoon. Over 600 nm, scattering due to particulate matter probably also contributes to the higher attenuation observed in Moorea. At short wavelengths ($\lambda < 515$ nm), reflectance spectra confirm the previous remarks. Reflectances are higher in Takapoto than in Moorea whereas an inverse trend is observed at longer wavelengths. These shapes are also explained by the stronger absorption in the blue-green part of the spectrum in Moorea, reducing the upwelling light flux and consequently $R^{\infty}(0-, \lambda)$ while increased scattering at long wavelengths leads to increased reflectances.

For further comparison with satellite data, the spectral values of the diffuse attenuation coefficient have to be transformed to correspond to the spectral bands of the concerned sensors. This was done by integrating the spectral irradiance data over

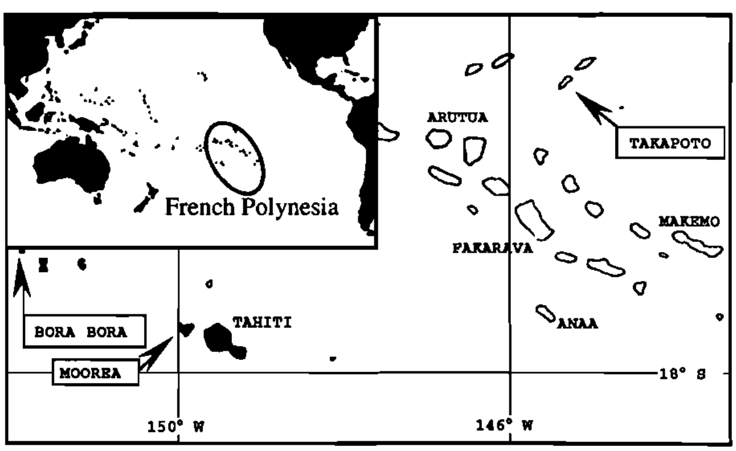

Figure 1. Location map of the islands of Moorea, Bora Bora and Takapoto.

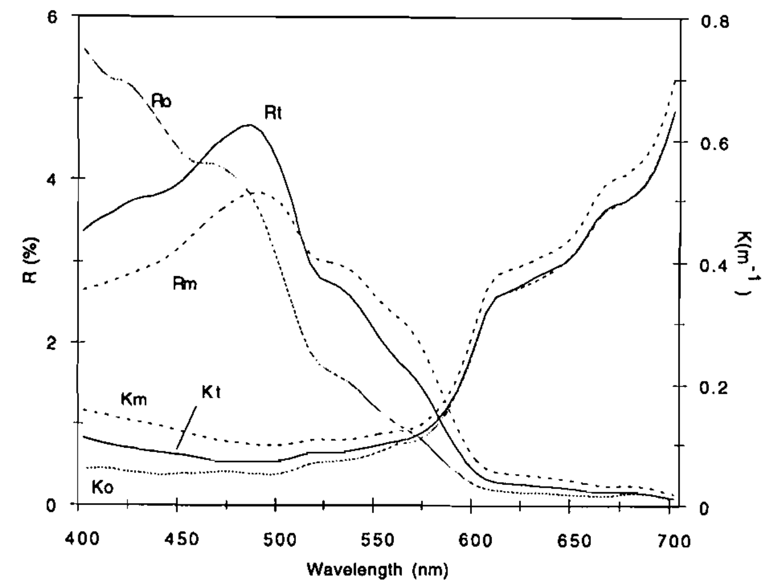

Figure 2. Mean spectra of the diffuse attenuation coefficient and reflectance measured in the ocean (Ko and Ro), in the lagoon of Takapoto (Kt and Rt) and in the lagoon of Moorea (Km and Rm).

the width of each band with respect to their spectral radiometric sensitivity according to:

$$E_{i,z}=\frac{\int_{\lambda_2}^{\lambda_1} E_d(\lambda, z)S_i(\lambda)d\lambda}{\int_{\lambda_2}^{\lambda_1} S_i(\lambda)d\lambda} \tag{4}$$

where $E_{i,z}$ is the integrated irradiance at depth z over the band i, S_i is the radiometric sensitivity of band i. These calculations were done for bands corresponding to Landsat TM-1 (450–520 nm), SPOT-XS1 (500–590 nm) and SPOT-XS2 (610–690 nm). The spectral radiometric sensitivity of each band was obtained from either Markham and Barker (1985) or from SPOT-image (1986), respectively.

Diffuse attenuation coefficients were then calculated for the three bands according to (3). Ratios for couples of bands were also computed for the 21 stations investigated (table 1).

Obviously, these data confirm the previous trends, viz. the stronger attenuation in the waters of Moorea compared to that of Takapoto and the greater clarity of the water in the ocean. At all stations the attenuation is lower in TM-1. However in the high island (Moorea), greater dissolved organic matter (DOM) and particle load in the waters lead to an increased attenuation at short wavelengths. This tends to reduce the differences between K(TM-1) and K(XS-1) which may sometimes be very close (see e.g., station 12 and station 15). The greatest variations are encountered for K(TM-1) as there is more than a factor of four between the lowest ($K=0{\cdot}054\,m^{-1}$ at station 6, very similar to the values found in the ocean) and the highest value ($K=0{\cdot}139\,m^{-1}$, station 14). The diffuse attenuation coefficient is very dependent of

Table 1. Diffuse attenuation coefficient in Landsat-TM-1, SPOT-XS-1 and SPOT-XS-2 bands calculated from the irradiance measurements in the ocean, in Moorea and, in Takapoto. Ratios of these coefficients.

Location	Station	K(TM-1) (m^{-1})	K(XS-1) (m^{-1})	K(XS-2) (m^{-1})	K(TM-1)/ K(XS-1)	K(TM-1)/ K(XS-2)	K(XS-1)/ K(XS-2)
Ocean	1	0·052	0·091	0·398	0·568	0·130	0·228
	3	0·054	0·099	0·421	0·544	0·128	0·236
	5	0·033	0·072	0·372	0·464	0·090	0·194
	7	0·055	0·086	0·369	0·638	0·149	0·234
	9	0·076	0·095	0·395	0·799	0·192	0·240
	Mean	0·054	0·089	0·391	0·603	0·138	0·226
	±SD	±0·013	±0·009	±0·019	±0·113	±0·033	±0·017
High island (Moorea)	2	0·117	0·137	0·497	0·850	0·235	0·276
	4	0·083	0·101	0·401	0·819	0·206	0·252
	6	0·054	0·085	0·370	0·635	0·146	0·231
	8	0·112	0·135	0·442	0·827	0·253	0·305
	10	0·109	0·125	0·413	0·868	0·263	0·303
	11	0·098	0·118	0·414	0·830	0·236	0·284
	12	0·120	0·135	0·451	0·890	0·266	0·299
	13	0·108	0·125	0·426	0·865	0·255	0·294
	14	0·139	0·156	0·461	0·892	0·302	0·339
	15	0·106	0·121	0·416	0·878	0·255	0·291
	16	0·109	0·126	0·423	0·865	0·258	0·298
	Mean	0·105	0·124	0·429	0·838	0·243	0·288
	±SD	±0·021	±0·018	±0·032	±0·068	±0·038	±0·027
Atoll (Takapoto)	17	0·113	0·147	0·498	0·768	0·226	0·294
	18	0·085	0·112	0·405	0·754	0·209	0·277
	19	0·072	0·103	0·395	0·701	0·182	0·260
	20	0·076	0·105	0·401	0·726	0·190	0·262
	21	0·067	0·092	0·381	0·721	0·175	0·242
	Mean	0·082	0·112	0·416	0·734	0·196	0·267
	±SD	±0·016	±0·019	±0·042	±0·024	±0·019	±0·018

the prevailing hydrological conditions. Attenuation is of course stronger for XS-2 mainly because of the strong absorption by the water at these wavelengths. K(XS-2) shows less variations than the other bands, the mean attenuation being very close for the three kinds of waters.

4. Optical properties of the water column from satellite data

A SPOT-1 multi-spectral image of the high island of Bora Bora (Society archipelago) has been processed to study the shallow water zone of the lagoon from remotely-sensed data (Image HRV1 No. 497 383, 5 June 1989). This island was chosen for several reasons: (1) its lagoon is wide, (2) the reef was supposed to have large homogeneous bottom zones, (3) an exhaustive field study of the lagoon had recently been conducted (Galzin *et al.* 1990) making comparison between image processing results and *in situ* observations possible, (4) since Bora Bora is a high island, the optical properties of its water are similar to those of Moorea.

A sub-scene containing the island (800 lines × 700 columns) has been extracted from the whole scene. To exclude the emerged zones (the island itself and the motus) the raw data were converted in a Hint, Intensity, Saturation image (HIS) and emerged pixels were eliminated by thresholding on the H and S images. This method provides better results in highly reflective bottoms than the simple use of XS-3. Deep zones were removed by thresholding on the I image and shallow water zones were determined by thresholding on XS-2. Hydrographic charts and data from Galzin *et al.* (1990) and Guilcher *et al.* (1969) showed that bottoms located deeper than approximately five metres were eliminated that way. Due to the very weak penetration in the water of the XS-3 band, it has not been considered in the following.

As this study only concerns shallow water zones, the radiances leaving the water represent the major part of the radiances measured at the sensor. For that reason and because of the small area covered by the lagoon of Bora Bora, no atmospheric corrections were performed. However, it should be noticed that the linearization of the data (2) can be regarded as a simplified atmospheric correction (Spitzer and Dirks 1987).

Once shallow water zones of the lagoon were isolated in XS-1 and XS-2, raw data were linearized in both bands according to:

$$X_i = \ln(XS_i - XS_{i\infty})$$

where XS_i is the radiance in band *i* and $XS_{i\infty}$ is the radiance measured in band *i* over a deep zone. $XS_{i\infty}$ was determined by calculating in each band a mean signal over deep ocean zones. At this stage, K(XS-1) and K(XS-2) or, at least the ratio K(XS-1)/K(XS-2) can be assessed from the image as proposed by Lyzenga (1981). For such estimations, 14 zones assumed to contain homogeneous bottoms at various depths were selected from aerial photographs, hydrographic charts and recent field study of Galzin *et al.* (1990) (figure 3). These zones contain from 600 to 2000 pixels. All zones have sandy carbonated bottoms except zone 11 to which corresponds a bottom with high massive coral cover (zone 11 is in two parts). As they have been determined independently and by different methods some zones are superimposed.

The scatterplots of the 14 zones in the $X_i - X_j$ spaces and the K(XS-1)/K(XS-2) as calculated from the symmetry axis are shown on figure 4. For each plot, the distribution of the points reveals the actual homogeneity of the bottom. Widely scattered points disprove the apparent homogeneity of some zones (e.g., zones 8, 11, ...).

With a mean value of 0·32 (not considering zones 8 and 11) the ratio K(XS-1)/K(XS-2) appears high compared to those obtained from *in situ* measurements (see table 1). Variations between zones are important and cannot be attributed only to the spatial variability of the optical properties of the waters. The quality of the test-zones is therefore essential in this method.

Instead of considering large zones, K(XS-1)/K(XS-2) can also be assessed from pairs of pixels at two different depths but with the same bottom. If the real depth of the bottom is known for the two pixels and with the proviso that tide corrections can be carried out, the diffuse attenuation coefficients can be estimated in each band. Otherwise the ratio K(XS-1)/K(XS-2) can be assessed directly. K(XS-1)/K(XS-2) calculated for 36 pairs of pixels show good uniformity, the mean ratio being equal to $0{\cdot}29\,m^{-1}$ (SD = 0·03) (figure 5) which is very close to what was found from *in situ* measurements in Moorea (a high island like Bora Bora) (see table 1). This method appears more practical than the previous one since it is very easy to conduct,

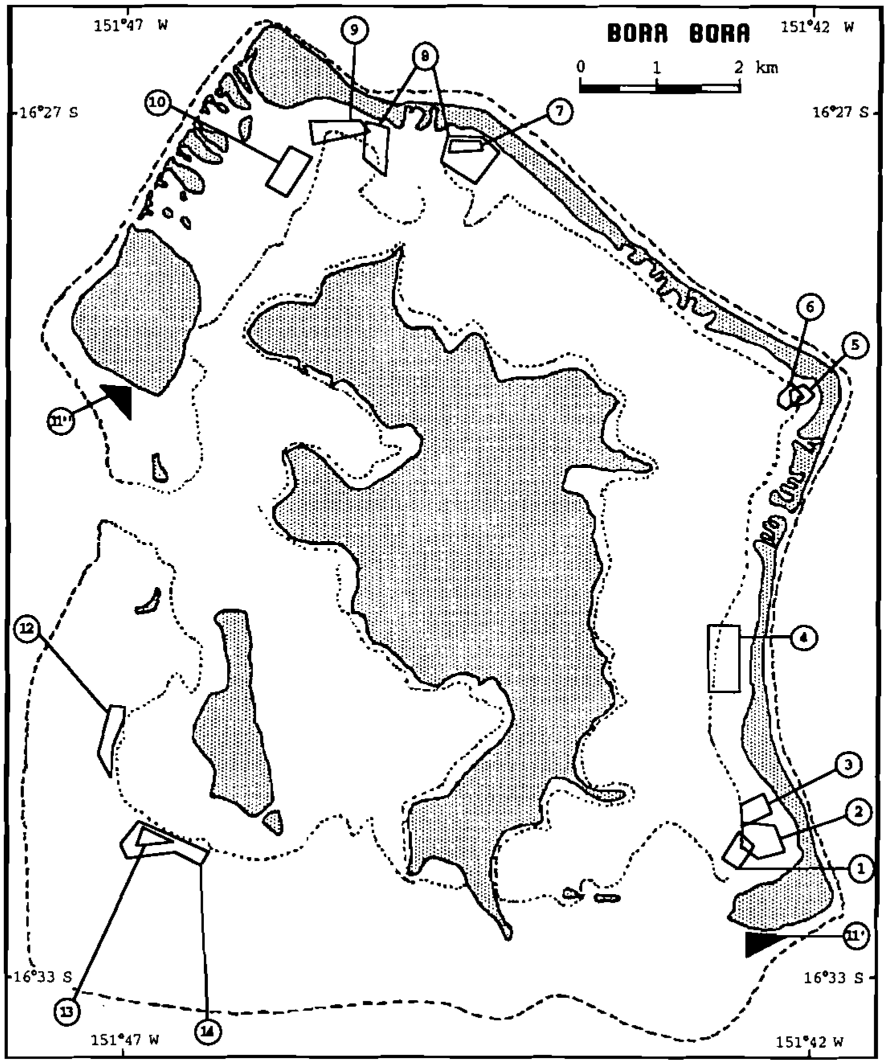

Figure 3. Location of the test zones in Bora Bora for the assessment of the ratio K(XS-1)/K(XS-2) from SPOT data.

provides better control of the data and is statistically more usable since zones with the requested characteristics are sometimes difficult to find.

5. Bottom mapping

Once the ratio K(XS-1)/K(XS-2) is known, the rotation of the axes leads to an image free of water column effects which can be regarded as being representative of the bottom itself. Such a rotation was carried out for a K(XS-1)/K(XS-2) ratio set to $0{\cdot}28\,m^{-1}$ involving a rotation of 15° 38′ (figure 6). In spite of the fact that the rotation results in a monochannel image, this resulting image is very informative on the organization of the reef. Schematically, radiances vary from white to black with decreasing reflectance of the bottom. Bright zones correspond to sand dominated

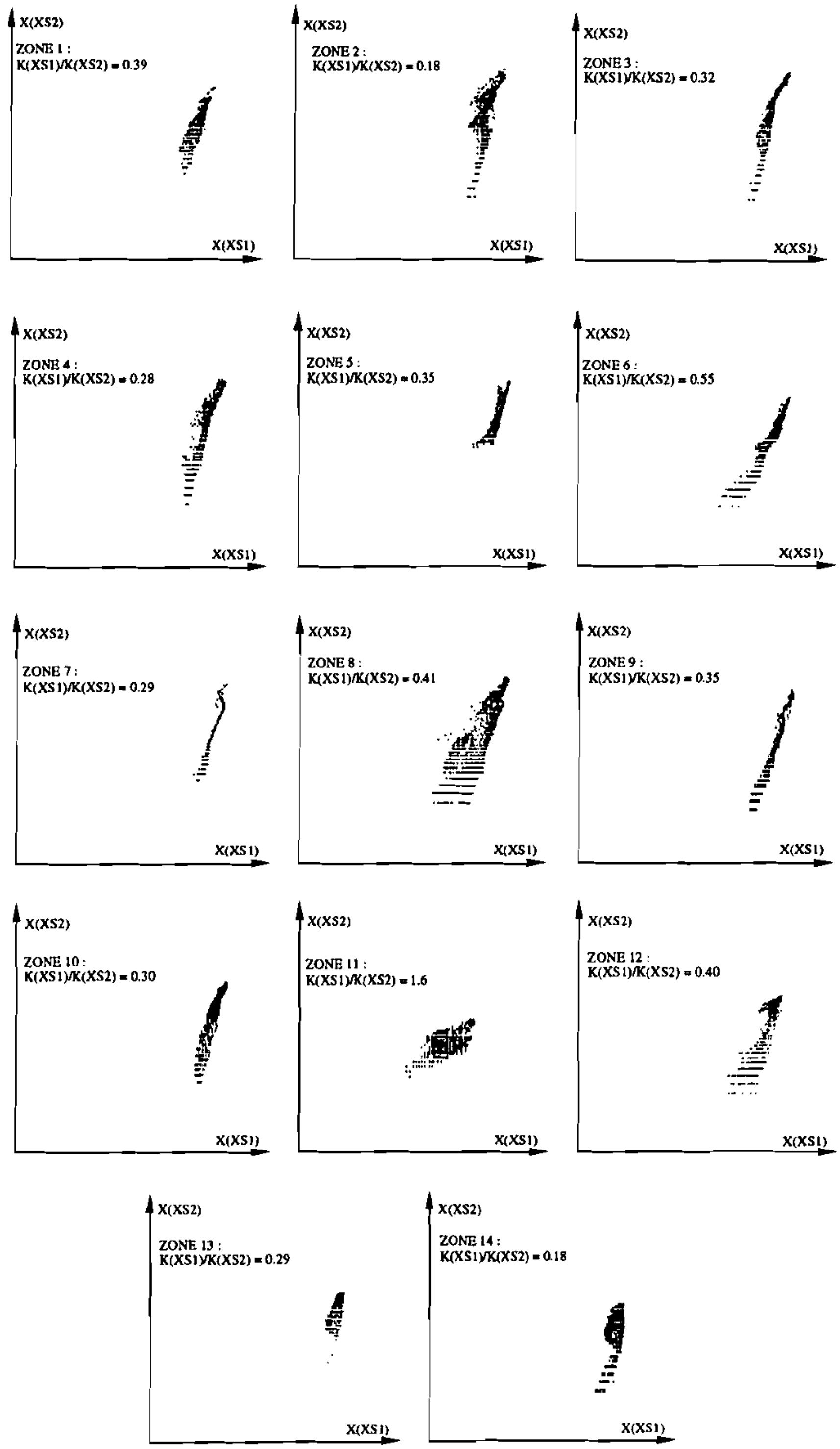

Figure 4. Scatterplots of the 14 test zones in the $X_i - X_j$ space. Values of K(XS-1)/K(XS-2) as given by the slope of the symmetry axis are indicated for each zone.

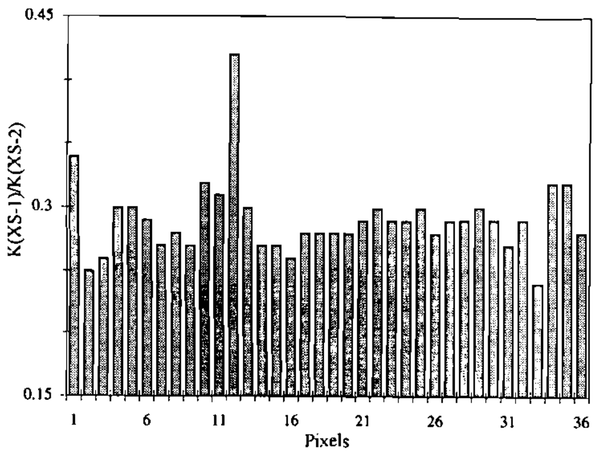

Figure 5. K(XS-1)/K(XS-2) estimated from 36 pairs of pixels in the Bora Bora image. Mean K(XS-1)/K(XS-2) = 0·29. Standard deviation = 0·03.

areas whereas the presence of live or dead organic build-up elements darkens the pixels. Sand dominated zones (marked (*a*) on figure 6) are easily identified in the north and east parts of the lagoon. High percentage massive coral cover zones (marked (*b*) on figure 6) are also well detected on the barrier reef just behind the reef front in the south and in the west, and south of the long eastern motu ('the garden of corals'). Corals are also well developed on both sides of the pass. Between these two

Figure 6. Image of the bottom in the shallow water zone of the lagoon in Bora Bora generated after axes system rotation.

extremes numerous intermediate situations can be found where corals, pavement (mostly relict eroded reef) and sand are intermixed in variable proportions. The southern and the south-western reef flat up to the pass correspond to such situations (marked (*c*) on figure 6). These areas show a complex organization linked to the geomorphological features of that part of the lagoon characterized by a strong hydrodynamism caused by ocean waves breaking over the reef front into the lagoon. These conditions are favourable to the development of branching corals. Mixed with various amount of sand they are probably responsible for most of the patterns observed on the south-western part of the image. The complex structure of that part of the Bora Bora lagoon is confirmed by the observations of Galzin *et al.* (1990). Another remarkable characteristic of the shallow water zones in Bora Bora is the large depression of the bottom in the north (marked (*d*) on figure 6) probably due to strong currents since at this location the lagoon is narrow.

This image is in very good agreement with the map proposed by Galzin *et al.* (1990) from aerial photographs and field observations. Despite the great richness of the image, the interpretation of the bio-geomorphological features of the lagoon is limited because it rests on a monoband image. A complete interpretation can be achieved if complementary data can be produced in order to work with a multi-band image but this is out of the scope of this paper.

6. Conclusion

As the radiances from the bottom are not directly usable in submerged coastal areas, it is sometimes difficult to make the most of remotely-sensed data. If bottom recognition is needed, the influence of the water column above the bottom may significantly modify the signal. The knowledge of the optical properties of the water may lead to the correction of this undesirable contribution. Unfortunately, optical data for coastal zones are rather scarce and are seldom applicable from one place to another. In this work, bottom mapping of the island of Bora Bora was obtained from remotely-sensed data through the use of a simple radiance model. Such a model allows the correction of the water column effects using the ratio of the diffuse attenuation coefficients in the wavebands used.

Attenuation can be assessed in different ways. The best estimations are obtained from *in situ* irradiance measurements. In the case of coral reef waters, our data clearly show that optical properties vary with the kind of island and the amount of emerged land. This terrestrial influence may strongly increase attenuation, mainly at short wavelengths and in TM-1- and XS-1-like wavebands.

When *in situ* measurements are not available, attenuation can also be assessed from remotely-sensed data. When homogeneous bottoms at various depths can be found on the image, attenuation can be estimated from zones or pairs of pixels. This latter method is easier to conduct and is more efficient. While great differences may exist between actual attenuation in the water and estimation from the image, such assessments must be carefully examined before being used in later image processing as the efficiency of the water column correction depends upon the accuracy of the K_i/K_j ratio.

In the study of Bora Bora island, the image processing by the linearization/rotation method gave satisfactory results. Unfortunately, as in this study the image processing uses two initial bands, the method results in a monoband image. This highlights the value of sensors having at least three bands in the visible with one in the blue part of the spectrum. Besides the better penetration of a blue channel and although particles and yellow substances may sometimes reduce this advantage, the benefit of a three-band sensor also rests on the improved channel combinations offered when working with three bands instead of two. For instance, a sensor with three bands in the visible may lead to a three-channel image corrected for water column effects which can then be easily processed by standard classification methods.

It should also be noticed that the spectral data and the methods presented here could be used for future visible sensors (e.g., SeaWiFS, OCTS, POLDER). However, this remark mainly concerns studies in oceanic zones as the spatial resolution of these sensors will generally not be appropriate in coral reefs.

Acknowledgments

Special acknowledgments are addressed to Professor Claude Payri and Professor André Morel for their help, advice and encouragement during this work. Professor Michel Ricard, Professor Bernard Salvat and Mr René Galzin are also thanked for providing logistical support for field measurements in Moorea. Mr Lionel Loubersac is acknowledged for providing image processing facilities at the Station Polynésienne de Télédétection in Papeete. Monique is thanked for help in English. I would also like to thank two anonymous referees for helpful comments.

References

Bina, R., Carpenter, K., Zacher, W., Jara, R. S., and Lim, J. B., 1978, Coral reef mapping using Landsat data: follow up studies. *Proceedings of the 12th International Symposium on Remote Sensing of Environment, Environmental Research Institute of Michigan May 1978* (Ann Arbor, Michigan: E.R.I.M.), pp. 2051-2070.

Blanchot, J., Charpy, L., and Le Borgne, R., 1989, Size composition of particulate matter in the lagoon of Tikehau atoll (Tuamotu archipelago). *Marine Biology*, **102,** 329-339.

Charpy, L., and Charpy-Roubaud, C. J., 1991, Particulate organic matter fluxes in a Tuamotu atoll lagoon (French Polynesia). *Marine Ecology Progress Series*, **71,** 53-63.

Delesalle, B., and Sournia, A., 1992, Residence time of water and phytoplankton biomass in coral reef lagoons. *Continental Shelf Research*, **12,** 939-949.

Galzin, R., Baldwin, J., Bonvallot, J., Chauvet, C., Fontaine-Vernaudon, Y., Gabrié, C., Holthus, P., Payri, C., and Planes, S., 1990, Etude du lagon de Bora Bora en vue de la création d'un parc marin. Action Délégation à l'Environnement, Rapport Antenne EPHE/Museum, 1990 RA 38.

Gordon, H. R., and Brown, O. B., 1974, Influence of bottom depth and albedo on the diffuse reflectance of a flat homogeneous ocean. *Applied Optics*, **13,** 2153-2159.

Guilcher, A., Berthois, L., Doumenge, F., Michel, A., Saint-Requier, A., and Arnold, R., 1969. Les récifs et lagons coralliens de Mopelia et de Bora Bora (îles de la Société). *Mémoires ORSTOM·38* (Paris: ORSTOM).

Jupp, D. L., Mayo, K. K., Kuchler, D. A., Heggen, S. J., and Kendall, S. W., 1981 a, Remote sensing by Landsat as support for management of the Great Barrier Reef. *Proceedings of the Second Australasian Remote Sensing Conference, Canberra, September 1981*, edited by P. Laut (Canberra: Australian Academy of Science), pp. 9.5.1-9.5.6.

Jupp, D. L., Mayo, K. K., Kuchler, D. A., Heggen, S. J., and Kendall, S. W., 1981 b, The Brian method for large area inventory and monitoring. *Proceedings of the Second Australasian Remote Sensing Conference, Canberra, September 1981*, edited by P. Laut (Canberra: Australian Academy of Science), pp. 6.5.1-6.5.5.

Jupp, D. L., Mayo, K. K., Kuchler, D. A., van D. Claasen, R. R., Kenchington, A., and Guerin, P. R., 1985, Remote sensing for planning and managing the Great Barrier Reef of Australia. *Photogrammetria*, **40,** 21-42.

LYZENGA, D. R., 1978, Passive remote sensing techniques for mapping water depth and bottom features. *Applied Optics*, **17**, 379-383.

LYZENGA, D. R., 1981, Remote sensing of bottom reflectance and water attenuation parameters in shallow waters using aircraft and Landsat data. *International Journal of Remote Sensing*, **2**, 71-82.

MARITORENA, S., MOREL, A., and GENTILI, B., 1994, Diffuse reflectance of oceanic shallow waters: influence of the water depth and bottom albedo. *Limnology and Oceanography*, **39**, 1689-1703.

MARKHAM, B. L., and BARKER, J. L., 1985, Spectral characterization of the LANDSAT Thematic Mapper sensors. *International Journal of Remote Sensing*, **6**, 697-716.

PHILPOT, W. D., 1989, Bathymetric mapping with passive multispectral imagery. *Applied Optics*, **28**, 1569-1578.

SOURNIA, A., and RICARD, M., 1976, Données sur l'hydrologie et la productivité du lagon d'un atoll fermé (Takapoto, îles des Tuamotu). *Vie et Milieu*, **26**, 243-279.

SPITZER, D., and DIRKS, R. W. J., 1987, Bottom influence on the reflectance of the sea. *International Journal of Remote Sensing*, **8**, 279-290.

SPOT-IMAGE, 1986. Guide des utilisateurs de données SPOT. CNES-SPOT-IMAGE (Editor), Toulouse, France.